ELSEVIER

Biomaterials 23 (2002) 4131–4141

Biomaterials

www.elsevier.com/locate/biomaterials

Silk matrix for tissue engineered anterior cruciate ligaments

Gregory H. Altman[a], Rebecca L. Horan[a], Helen H. Lu[a], Jodie Moreau[a], Ivan Martin[b], John C. Richmond[c], David L. Kaplan[a,*]

[a] *Bioengineering Center, Department of Chemical and Biological Engineering, Tufts University, 4 Colby Street, Medford, MA 02155, USA*
[b] *Department of Surgery, Research Division, University Hospital Basel, 4031 Basel, Switzerland*
[c] *New England Medical Center, Department of Orthopaedics, Boston, MA, USA*

Received 30 January 2002; received in revised form 1 April 2002; accepted 26 April 2002

Abstract

A silk-fiber matrix was studied as a suitable material for tissue engineering anterior cruciate ligaments (ACL). The matrix was successfully designed to match the complex and demanding mechanical requirements of a native human ACL, including adequate fatigue performance. This protein matrix supported the attachment, expansion and differentiation of adult human progenitor bone marrow stromal cells based on scanning electron microscopy, DNA quantitation and the expression of collagen types I and III and tenascin-C markers. The results support the conclusion that properly prepared silkworm fiber matrices, aside from providing unique benefits in terms of mechanical properties as well as biocompatibility and slow degradability, can provide suitable biomaterial matrices for the support of adult stem cell differentiation toward ligament lineages. These results point toward this matrix as a new option for ACL repair to overcome current limitations with synthetic and other degradable materials. © 2002 Published by Elsevier Science Ltd.

Keywords: Silk; Fibroin; Ligament; Bone marrow stromal cells; Stem cells; Tissue engineering

1. Introduction

The high incidence of anterior cruciate ligament (ACL) failures, coupled with the absence of adequate clinical options to restore full knee joint function, have prompted consideration of tissue engineering strategies. ACL ruptures can result in severe limitations in mobility, pain and discomfort, and inability to participate in sports and exercise. The ACL has poor healing capabilities, and no surgical procedure can reliably and completely restore function due to autograft donor site morbidity leading to pain and tendonitis, long recovery periods, and muscle atrophy [1–4]. Tissue engineering can potentially provide improved clinical options in orthopaedic medicine through the in vitro generation of biologically functional tissues for transplantation at the time of injury or disease [5].

The knee joint geometry and kinematics related to ACL structure must be incorporated into any design strategy if a tissue engineered ACL generated in vitro is to successfully stabilize the knee and function in vivo. A mismatch in the ACL structure–function relationship would result in graft failure. Our hypothesis is that mechanical signals applied in vitro to a growing ACL will induce the formation of the required structural and functional features to mimic performance requirements in vivo. This hypothesis is based on two principles related to ACL structure and function: (1) the ACL helical geometry allows individual fiber bundles to remain isometric during flexion extension, thus equally distributing the load throughout the ACL and stabilizing the knee [6], and (2) ACL mechanical properties, particularly linear stiffness and ultimate tensile strength (UTS), must be incorporated into the matrix design if host tissue ingrowth and constant biological remodeling are to be the primary means of knee joint stabilization over the long term [7]. The objective of the study was to engineer a mechanically and biologically functional matrix for ACL tissue engineering. Proper matrix design is essential to a successful tissue engineered ACL and provides a foundation upon which to explore mechanics and biological function.

*Corresponding author. Tel.: +1-617-627-3251; fax: +1-617-627-3231.
E-mail address: david.kaplan@tufts.edu (D.L. Kaplan).

0142-9612/02/$ - see front matter
PII: S0142-9612(02)00156-4

In our prior work we demonstrated that mechanical forces applied to 3D collagen gels can selectively induce the differentiation of adult stem cells into ligament-like cells and tissues based on molecular, cellular and tissue markers [8]. In the present study we extend this concept by employing a novel matrix that can provide mechanical integrity to match ACL performance requirements over a suitable time period to permit slow ingrowth of new tissue. We propose the use of a novel silk fiber-based matrix in combination with a wire-rope design to mirror the ACL in UTS and linear stiffness. Silk was selected from the array of alternative synthetic and natural fibers for this application because it is the only protein-based fiber that: (1) can match the required mechanical properties of an ACL, (2) is biocompatible when properly prepared [9], (3) avoids bioburdens associated with mammalian-derived materials, (4) maintains mechanical tensile integrity in vitro in tissue culture conditions and (5) exhibits slow degradation in vivo [10] allowing for adequate time for host tissue infiltration and eventual stabilization. Silk has been used clinically as suture material for decades and has gained renewed interest as a biomaterial for tissue engineering [9,11–13].

We report on efforts to prepare and optimize a silk-fiber matrix with mechanically and biologically relevant properties with respect to the needs for a tissue engineered ACL. We report a novel preparation method for the matrix as well as initial evaluation of adult human progenitor bone marrow stromal cell (BMSC) attachment, proliferation and ligament specific differentiation on this silk fibroin matrix. The results support the conclusion that silk fiber matrices, when properly prepared, can provide a suitable biomaterial matrix for support of adult stem cell differentiation toward ligament lineage. When these results are combined with the mechanical properties and slow degradability of silk, this protein matrix offers a unique opportunity to overcome clinical limitations with current ACL repair options.

2. Materials and methods

2.1. Preparation of silk fibers

White Brazilian raw *Bombyx mori* silkworm fibers of size 20/22 (according to the manufacturer) were obtained through Rudolp-Desco Co. (Englewood Cliffs, NJ). The average diameter of the silkworm fibers ($N = 9$ fibers, 3 measurements were taken from each fiber) was determined optically using an inverted microscope (Axiovert S100, Zeiss, Germany), and digital image analysis: 3CCD color video camera (DXC-390, Sony, Tokyo, Japan), a frame grabber card (CG-7 RGB, Scion, Frederick, MD) and Scion-Image software version 1.9.1. The fibers were processed by extraction of sericin, the glue-like protein coating the native silk fibroin, using an aqueous solution containing 0.02 M Na_2CO_3 and 0.3% Ivory detergent as previously described [11]

Bundles of 5 or 10 parallel fibers, 1.4 m in length held within a custom-designed extraction rack to keep individual fibers or groups of fibers in constant tension, were extracted in a 160 l custom-designed 304 stainless-steel bath with recirculating flow (75 l/min). Sericin removal, fiber UTS (N) and linear stiffness (N/mm) were characterized as a function of extraction temperature up to 90°C for a 60-min processing period by scanning electron microscopy (SEM) and single-pull-to-failure mechanical analysis.

2.2. Silk fiber wire-rope design and model

To reduce the high linear stiffness associated with single extracted fibroin fibers, a wire-rope design was chosen for multi-fiber matrices. Costello's equation [14] for a 3-strand wire rope was derived to predict mechanical properties of a multi-level silk fibroin matrix that could mirror the ACLs stress–strain curve (Table 1). The model was used to eliminate the time associated with experimental trial and error in determining an appropriate matrix geometry. The model takes into account extracted silk fibroin material properties and the desired matrix geometric hierarchy to predict the overall strength and stiffness of the matrix as a function of pitch angle.

The material properties required for input into the model of a single extracted silk fiber included fiber diameter, modulus of elasticity, Poisson's ratio (0.4), and UTS. Geometric hierarchy was defined as the number of twisting levels in a given matrix level. For description purposes, five levels of geometric hierarchy were defined (e.g., fiber, bundle, strand, cord, or matrix (e.g., the ligament)); an infinite number of levels exist. An example of numerical representation of a 6-cord matrix could be defined as $30(0) \times 6(2) \times 3(2) \times 6(0) \times 1$ indicating 30 fibers in 1 bundle, 6 bundles in 1 strand, 3 strands in 1 cord and 6 cords in 1 ACL matrix. The

Table 1
Mechanical properties of 6 cord wire-rope silk matrix, $N = 5$, theoretical properties of the same matrix with only parallel fibers, and the human ACL taken from Woo et al. [38]

	UTS (N)	Stiffness (N/mm)	Yield Pt. (N)	Elongation (%)
Silk matrix	2337±72	354±26	1262±36	38.6±2.4
Parallel silk matrix	2214	1740	1274	26.5
Human ACL	2160±157	242±28	~1200	~33

numbers in parentheses indicate the number of twists per centimeter (tw/cm) at that level. Each level was further defined by (1) the number of bundles of fibers twisted about each other and (2) the number of fibers in each bundle of the first level twisted. The matrix hierarchy is schematically depicted in Fig. 1. The model assumes that each bundle of multiple fibers act as a single fiber with an effective radius determined by the number of individual fibers and their radii. Thus, the model discounts friction between the individual fibers due to the anticipated limited impact of this process at a relatively high pitch angle. Several strands consisting of six bundles of 10 fibers were used to verify the theoretical model and predicted outcomes; 0, 2, 3, and 5 tw/cm were imparted to the strands and UTS and linear stiffness determined as a function of bundle pitch and compared to the theoretical predictions.

2.3. ACL silk matrix fabrication

The model was used to derive an applicable geometry within manufacturing constraints that would mirror ACL mechanical properties, aid in cell seeding and support tissue ingrowth. The number of fibers and geometry were selected such that the silk matrix was similar to the ACL in UTS, linear stiffness, yield point and percent elongation at break.

2.4. Cells

Human BMSCs were isolated and culture expanded as previously described [8]. Briefly, human bone marrow aspirates obtained from consenting, non-smoking donors $\leqslant$25 years of age (Clonetics-Poietics, Walkersville, MD) were resuspended in Dulbecco's Modified Eagle Medium (DMEM) supplemented with 10% fetal bovine serum (FBS), 0.1 mM non-essential amino acids, 100 U/ml penicillin, 100 mg/l streptomycin (P/S), and 1 ng/ml basic fibroblast growth factor (bFGF) (Life Technologies, Rockville, MD) and plated at 8–10 μl aspirate/cm^2 in tissue culture flasks. BMSCs were selected based on their ability to adhere to the tissue culture plastic after 10–12 days in culture; non-adherent hematopoietic cells were removed during medium replacement [8]. Medium was changed twice per week thereafter. When primary BMSCs became near confluent, they were detached using 0.25% trypsin/1 mM EDTA and replated at 5×10^3 cells/cm^2. First passage (P1) BMSCs were trypsinized and frozen in 8% DMSO/10% FBS/DMEM for future use.

2.5. Matrix cell seeding

A custom-designed Teflon seeding chamber was designed. The chamber has 24 wells, each 3.2 mm wide by 8 mm deep by 40 mm long (1 ml total volume) machined into a Teflon block designed to fit within a 150 mm petri dish. Frozen P1 BMSCs were defrosted, plated at 5×10^3 cells/cm^2 (P2), trypsinized when near $\sim$85% confluency, and used for matrix seeding within the Teflon wells. Sterilized (ethylene oxide) silk cords and bundles were seeded with cells in the customized seeding chambers to minimize the cell to medium volume and increase cell–matrix contact.

Single ACL matrix fibroin cords of geometry $30 \times 6(3) \times 3(3) \times 6$ were tied together with 2–0 Ethibond polyester sutures (Ethicon, NJ) using a combination of a whip-stitch and square knot; cords were 3 cm in length between the sutures. Cords were seeded with 3.3×10^6 cells in 1 ml of cell culture medium without bFGF as follows: (1) sterilized cords were placed within the wells of the steam sterilized Teflon block, (2) 250 μl of the cell suspension (1×10^6 cells/ml) was added to wells containing cords and incubated at 37°C and 5% CO_2 for 30 min, (3) the cords were rotated 90° followed by a second 250 μl addition of the cell suspension and a 30 min incubation period; the procedure was repeated twice more for a total of 2 h to uniformly seed the cords. Following seeding, the cords were cultured independently in an appropriate amount of cell culture medium for 0 (immediately post-seeding), 1, 7, and 14 days ($N = 2$ per time point for SEM and 2 for DNA) and cell morphology, growth and marker expression ($N = 3$ at day 14) assessed.

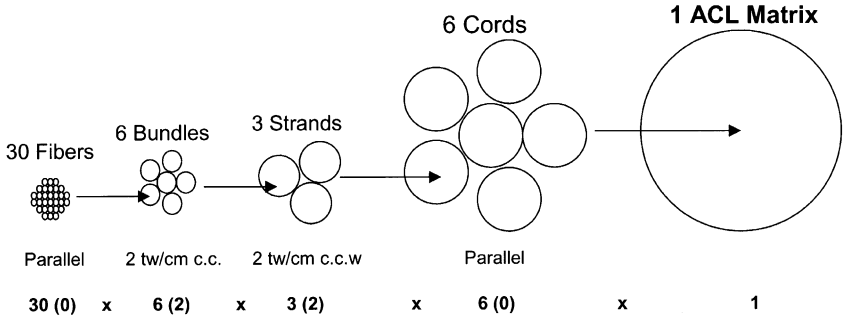

Fig. 1. Schematic of an ACL 6-cord matrix hierarchy.

2.6. Silk integrity study

To test the mechanical integrity of silk fibroin in physiologic cell culture conditions, bundles of 30 extracted silk fibers 3 cm between sutures were prepared. Bundles were seeded as described above using a 1×10^6 cells/ml cell suspension and cultured for 1, 7, 14 and 21 days ($N = 8$ per time point); otherwise identical non-seeded matrices were generated for use as controls. Single pull-to-failure mechanical analysis was performed as described above by clamping directly on the knotted sutures eliminating the need for molded epoxy ends. Matrices were saturated with cell culture medium throughout the testing procedure.

3. Analytical methods

3.1. Mechanical analysis

Mechanical testing was performed using a servohydraulic Instron 8511 (Instron, Canton, MA) tension/compression system with Fast-Track software. Single pull-to-failure analysis was performed on: (1) single bundles of 10 parallel fibers ($N = 8$ per extraction condition) used for characterization of the extraction process, (2) strands (of varying tw/cm) of 6 bundles containing 10 fibers each used for model verification ($N = 5$ per pitch angle), (3) single cords of the ACL matrix ($N = 5$), and (4) bundles of 30 parallel fibers for silk integrity testing in tissue culture conditions ($N = 8$ per time point). Bundle, strand and cord ends were embedded in an epoxy mold to generate constructs 3 cm in length between grip anchors. Fatigue analysis was performed on single ACL matrix cords. Since cord is designed to be in parallel, cord data was extrapolated to represent the 6-cord ACL matrix. Single pull-to-failure testing was performed at a strain rate of 100%/s and data were analyzed using Instron Series IX software. Cycles to failure at UTS, 1680N, and 1200N ($N = 5$ for each load) were determined using a H-sine wave function at 1 Hz generated by Wavemaker32 ver. 6.6 (Instron, MA). Fatigue testing was conducted in neutral phosphate buffered saline (PBS) at 23°C. Samples were prepared and stored for no more than 7 days at room temperature prior to testing.

3.2. Scanning electron microscopy

The matrices were harvested at timed intervals, washed with 0.2 M sodium cacodylate buffer, fixed overnight in Karnovsky fixative, dehydrated through an ethanol series and left to dry in Freon overnight. The samples were sputter-coated with Au using a Polaron SC502 Sputter Coater (Fison Instruments), and imaged at 15 keV with a JEOL JXA 840 SEM.

3.3. DNA analysis

Cell proliferation was quantitatively measured via total cellular DNA using the Picogreen dsDNA Quantitation Assay (Molecular Probes, Eugene, OR). At the designated time points (1, 7, and 14 days post-seeding), samples were harvested, rinsed in PBS, vortexed for 60 s in 0.05% Triton-X and incubated at room temperature for 2 days, diluted 1:5 with Picogreen reagent and total DNA quantified following a protocol supplied by the manufacturer.

3.4. Real-time quantitative reverse transcriptase polymerase chain reaction

Three seeded identical 3 cm cords cultured for 14 days were harvested, rinsed in PBS and homogenized in 1.5 ml of Trizol (Life Technologies, Rockville, MD) using a mini-bead beater (Biospec, Bartlesville, OK). Total RNA was isolated and real-time RT-PCR performed with primers designed to collagen types I, II and III, tenascin-C and the housekeeping gene, GAPDH as previously described [8,15].

4. Results

The influence of extraction protocols on mechanical properties was assessed using temperatures from 22°C to 90°C and times from 15 to 60 min. The 90°C for 60 min regime was found most suitable in removal of the contaminating sericin (Fig. 2) while preserving the majority of the fibroin's mechanical integrity within acceptable limits (Fig. 3). Extraction of sericin from the silk fibers, 52 ± 8 μm in diameter, altered the diameter and appearance of the fibers as observed by SEM. A smoother fiber surface with average diameter of 38 ± 5.6 μm resulted after extraction for 60 min at 90°C (Fig. 2C). Extraction at 90°C for 60 min completely removed sericin revealing the underlying silk fibroin with individual diameters ranging from 5 to 20 μm (Fig. 2C). A single fiber exhibited a significant ($p < 0.05$, paired Students t-test) 15.2% decrease in UTS (1.03 ± 0.04 to 0.88 ± 0.1 N) and a significant 28.3% decrease in linear stiffness (from 1.91 ± 0.04 to 1.37 ± 0.21 N/%) as a function of extraction and sericin removal at 90°C for 60 min when compared with the raw fibers (Fig. 3).

The computational model accurately predicted the UTS up to 5 tw/cm and stiffness up to 2 tw/cm for the given wire-rope bundle geometries (Fig. 4). When challenged with a relatively low matrix pitch angle (e.g., high number of tw/cm), the model overestimated stiffness, failing to accurately predict it beyond 2 tw/cm.

A 6-cord matrix (versus a single cord, larger diameter matrix) was chosen for several reasons: (1) ligament

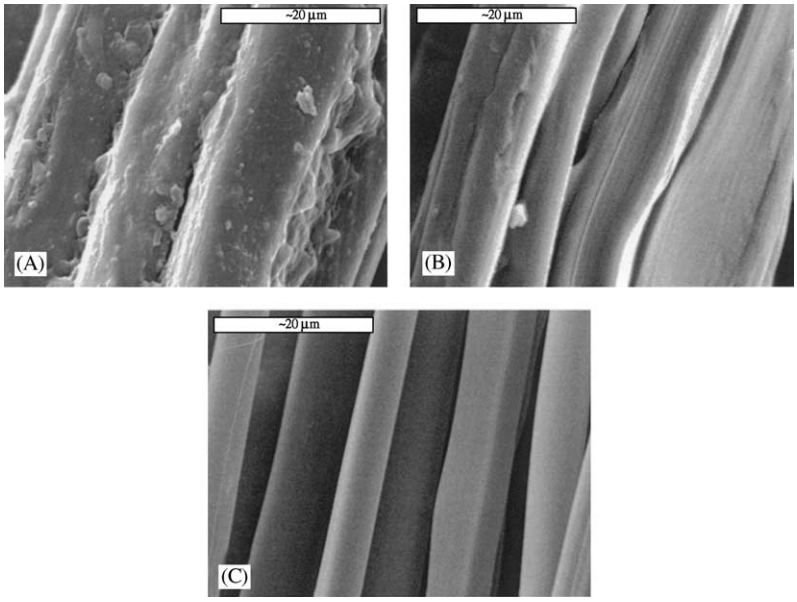

Fig. 2. SEM images illustrating the changes in surface texture of a single fibroin fiber prepared by different extraction procedures; original fiber (A), extraction for 60 min at 37°C (B), and extraction for 60 min at 90°C (C). Scale bars = 20 µm.

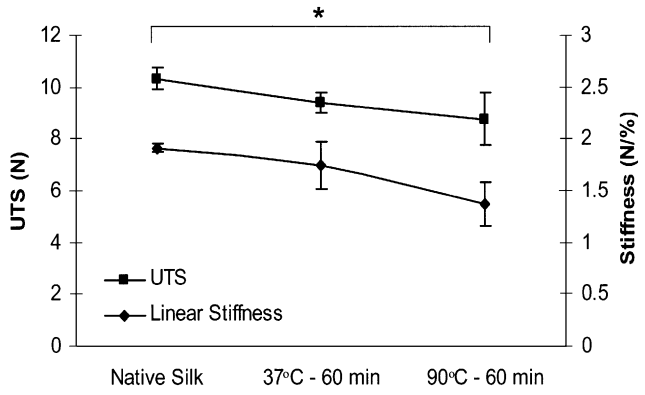

Fig. 3. Mechanical properties (mean ± standard deviation) of the silk fibers (bundle of 10) ($N = 8$ per extraction condition) prepared using the extraction conditions described in Fig. 1. UTS = ultimate tensile strength. Asterisk indicates a statistically significant (t-test, $P < 0.05$) decrease in strength at 90°C and 60 min extraction conditions compared to native fibers.

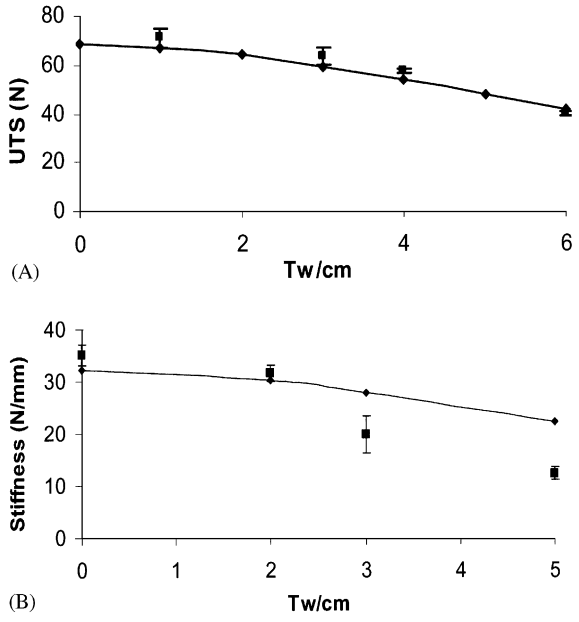

Fig. 4. Empirical results ($N = 5$ per pitch angle) of mechanical properties at 0, 2, 3, and 5 tw/cm compared to theoretical model predictions (smooth line); (A) estimates of UTS; (B) estimates of stiffness; (tw) twist.

graft tensioning at the time of surgical reconstruction requires a single or even a number of cords prior to permanent fixation within the knee to ensure load is distributed equally throughout the matrix; (2) the 6-cord matrix (versus a 1, 2 or 4 cord graft) offers the greatest surface area to enhance cell seeding and density and promote host tissue ingrowth and development while decreasing nutrient and metabolite mass-transfer limitations; (3) given in vivo anchoring constraints, e.g., 8–10 mm diameter bone tunnels, the 6-cord matrix was geometrically optimal (i.e., provides greater ligament–bone contact area than a 4 cord matrix). A matrix in excess of 6 cords, while providing increased surface area, was a concern due to the introduction of difficulties associated with matrix tensioning and anchoring.

Several pilot-scale manufacturing and design constraints limited the number of possibilities for the geometries of the 6-cord matrix: (1) the twisting machine was configured to anchor 6 equally spaced fibers, bundles, strands or cords; therefore, equally spaced fibers, were limited to 180°, 120° or 60°, and (2) an equal

number of hierarchical levels twisted in opposite directions were required for cord stability. With the manufacturing limits of available equipment, a cord geometry encompassing 3 strands of 6 bundles each resulted in the most stable rope configuration. The model was used to identify geometries (i.e., the number of fibers per bundle and the number of twists per level) that resulted in the targeted mechanical properties. Two 6-cord designs, $25 \times 6 \times 3 \times 6$ and $30 \times 6 \times 3 \times 6$, were pursued. The geometrical hierarchy of the matrix that best mirrored the ACL was as follows: 1 ACL prosthesis = 6 parallel cords; 1 cord = 3 twisted strands (3 tw/cm counter clockwise); 1 stand = 6 twisted bundles (3 tw/cm clockwise); 1 bundle = 30 parallel extracted fibers. A single cord of the 6-cord matrix is shown in Fig. 5. The resulting ACL matrix contained 3240 pre-extracted fibers with a combined cross-sectional area of 3.67 mm^2 and could tightly fit within a 4 mm diameter bone tunnel.

The selected silk matrix exhibited mechanical properties (Fig. 6A; Table 1) comparable to those of the native human ACL (Table 1): UTS of 2337 ± 72 N, stiffness of 354 ± 26 N/mm, yield point of 1262 ± 36 N, and $38.6 \pm 2.4\%$ elongation at break. Regression analysis of matrix fatigue data (Fig. 6B), when extrapolated to physiological load levels (400 N) [16] to predict number of cycles to failure in vivo, indicated a matrix life of 3.3 million cycles.

Matrix fabrication resulted in uniform and repeatable mechanical properties (Fig. 6A, Table 1); UTS and stiffness deviated from the mean by only 3.1% and 7.3%, respectively. This matrix design provided the desired mechanical properties while minimizing required intra-articular space (99 versus 1357 mm^3 for a native ACL assuming an average diameter of 8 mm and length of 27 mm), allowing room for the ingrowth of host tissue. The wire–rope geometry compared to an equivalent parallel fiber matrix, reduced matrix linear stiffness by 80% without significantly affecting the UTS of the 6-cord matrix (Table 1).

The silk fibers retained mechanical tensile strength over 21 days in tissue culture conditions (Fig. 7). No statistically significant changes in UTS were observed when comparing seeded and non-seeded matrices. Human BMSCs readily adhered (Fig. 8B), spread and grew on the silk fiber matrix after 1 day (Fig. 8C) in culture and formed cellular extensions to bridge neighboring fibers. A uniform cell sheet and possible ECM covering the fibrous construct was observed by 14 days of culture (Fig. 8D). Measures of total DNA, from 2 cords per time point, confirmed BMSC proliferation on the silk with the highest amount of DNA measured after 14 days in culture (Fig. 9). Real-time RT-PCR assessment of 3 seeded cords cultured for 14 days indicated ligament-specific marker expression (e.g., collagen types I and III, tenascin-C) by the cultured BMSCs (Fig. 10). Collagen types II and bone sialoprotein, as markers of cartilage and bone specific differentiation, respectively, were negligibly expressed. Furthermore, the ratio of collagen type I expression to collagen type III was 8.9:1, consistent with that of cruciate ligaments [17].

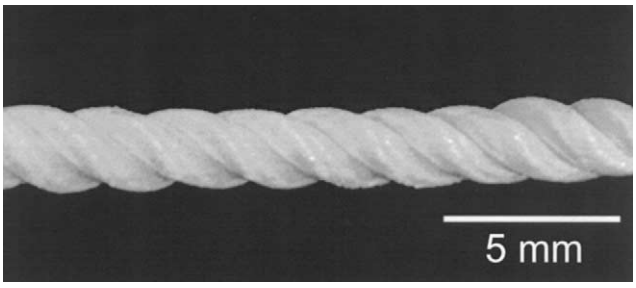

Fig. 5. Photograph of a single silk fibroin cord containing a total of 540 individual fibers. Six parallel cords are used to generate the ACL matrix.

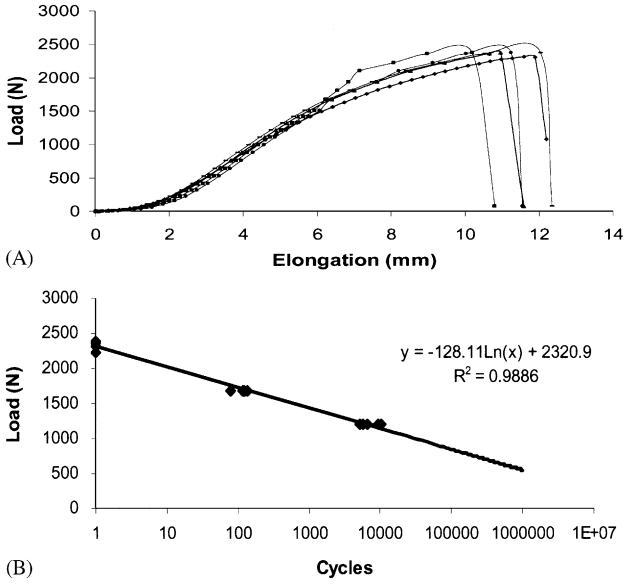

Fig. 6. Load-elongation ($N = 5$) (A) and cycles to failure ($N = 5$ per load) (B) histograms for the silk 6-cord matrix. The fatigue data trend-line is extrapolated to a physiologically relevant cyclic load of 400 N.

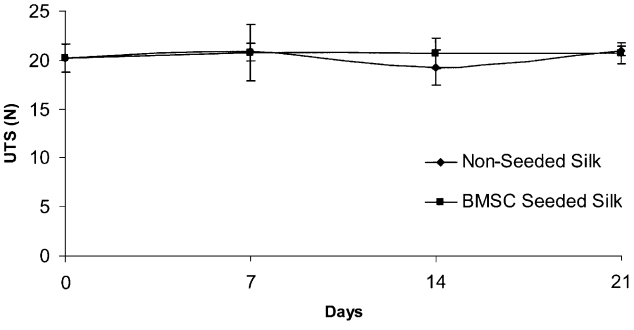

Fig. 7. Effect of cell culture conditions on the mechanical properties of BMSC seeded and non-seeded silk fiber bundles (30 fibers per bundle) during 21 days.

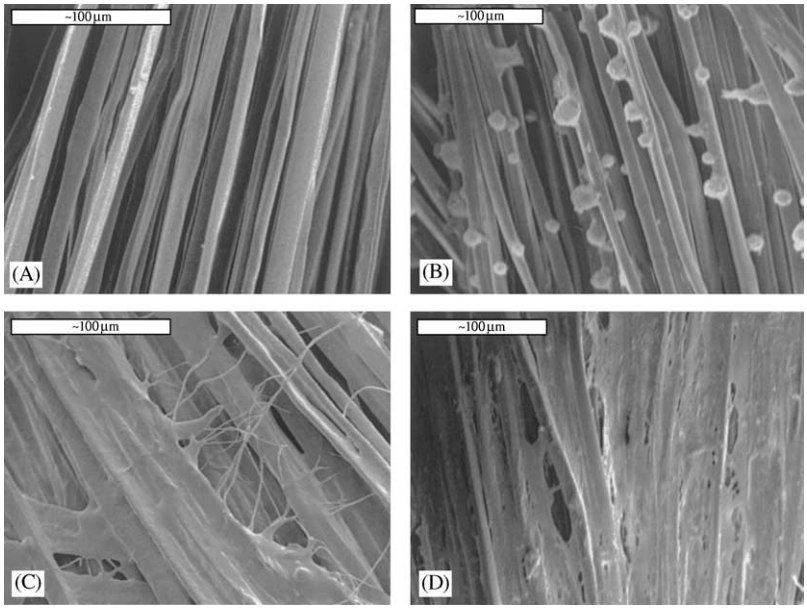

Fig. 8. SEM showing adherence, proliferation and cell sheet formation by human BMSCs on the silk cord matrix prior to seeding (A), time 0 following seeding (B), 1 day (C), and 14 days (D). Scale bars = 100 μm.

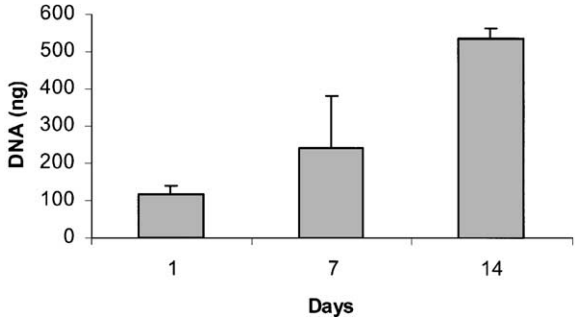

Fig. 9. DNA content during 14 days of growth of human BMSCs on the silk cord matrix. Standard deviations are shown from 2 cords per time point. The highest level of DNA was observed after 14 days.

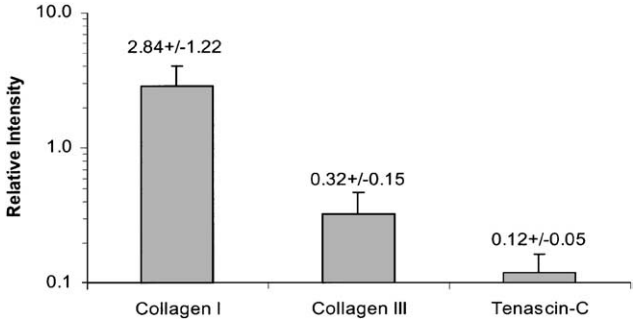

Fig. 10. mRNA expression of ligament markers by human BMSC cultured for 14 days on the silk cord. Levels, quantified using real-time RT-PCR, are normalized to the housekeeping gene, GAPDH.

5. Discussion

Patellar or hamstring tendon autografts are utilized in approximately 90% of ACL reconstructions. While autologous bone–patellar tendon–bone grafts and 4-cord hamstring grafts utilizing the gracilis and semi-tendinosus tendons and enhanced anchoring techniques provide good surgical outcomes stabilizing the knee, tendon donor site morbidity results in months of rehabilitation, pain, tendonitis and muscle atrophy [18–20]. As a result, complete return to pre-injury activity levels occurs for only 85% of patellar tendon and ~70% of hamstring tendon recipients during 12–18 months [3,4].

Tissue engineering provides an alternative approach to generate biologically and mechanically relevant autologous ligament grafts by combining cell sources such as adult bone marrow stromal cells (BMSC) with a biomaterial matrix. In combination with appropriate environmental signals BMSCs can be directed toward ligament fibroblasts in vitro [8]. Our hypothesis is that mechanical stimulation that is physiological in nature but applied in vitro can lead to ligament formation in a bioreactor system [8]. To evaluate this hypothesis, novel biomaterials with biologically relevant traits that can withstand a rigorous and dynamic mechanical environment in vitro and in vivo are required. Traditional materials such as non-degradable synthetics failed to promote directed and organized host-tissue ingrowth in vivo due to mismatches in stress–strain characteristics. The lack of the continual biologic remodeling limited ACL integrity to that of the material's fatigue life [21–23]. Degradable biomaterials such as collagen and some synthetic polymers, while offering good biological characteristics and accelerated degradation rates in tissue culture conditions, fail to provide adequate mechanical function in a demanding mechanical environment over a sufficient time frame to allow

for the formation of new matrix to sustain the tissue [24,25]. Several collagen-based scaffolds, including collagen fibers embedded in a collagen gel or in a PLA composite, as well as the use of various cross-linking methods [26,27], were examined as ACL replacements in a rabbit model. The protein-synthetic polymer composite was employed to slow down the degradation rate observed for the collagen-based scaffolds. For both the collagen and collagen–PLA composite, less than half of the ligament prostheses remained intact after 4 weeks in vivo or before neoligament tissue could stabilize the matrix [25]. Attempts to slow the degradation rate of collagen fibers in vivo, such as by cross-linking with gluteraldehyde versus carbodiimide, adversely affected biocompatibility by generating a stronger immune response and fibrous encapsulation [28].

Silk fibers offer a novel alternative to traditional native and synthetic non-degradable and degradable biomaterials by combining the optimal traits of both groups. The US Pharmacopia defines an absorbable material as one that loses "most of its tensile strength within 60 days" in vivo. By this definition, silk is correctly classified as non-degradable. However, according to the literature silk is degradable over longer time frames as a function of proteolytic degradation usually mediated by an in vivo foreign body response [29–32]. Several studies detail silk degradation in vivo with variable rates dependent on the model and implantation site [10,29,32–34]. In general, silk fibers lost the majority of their tensile strength within 1 year in vivo, and failed to be recognized in the implantation site within 2 years. Silk lost 55% of its tensile strength when circumferentially implanted subcutaneously in rats over a 6 week period [10]. Bucknall et al. [32] reported an 83% loss in silk fiber tensile strength after 10 weeks in vivo when implanted subcutaneously in rats. Lam et al. [29] was unable to detect silk as well as a foreign body response 24 weeks following implantation in the abdominal muscle layer in rats. Salthouse et al. [33] observed a reduction in the number of silk filaments and the overall diameter of silk sutures 42 days following implantation in the cornea, sclera and ocular muscle of the rabbit and complete absorption within 90 days in vivo. Prostlethwait [34] observed fragmentation of silk sutures 4 weeks in vivo and an 80% decrease in strength at 12 weeks in the rabbit abdominal wall muscle. In vitro, silk was proteolytically degraded by protease cocktails [13] and chymotrypsin [35].

Silk fibers are also attractive due to their impressive mechanical properties (>1 GPa) [36], can be metabolized in vivo to biocompatible amino acids, can be genetically designed if needed to optimize specific structural features [37], and offer diversity in amino acid side chain chemistries for facile coupling of selective growth and adhesion factors [11]. Silks have been used as substrates for the culture of anchorage-dependent mammalian cells with efficiency comparable to collagen [9], as a template for osteogenic tissue formation [11], and as burn wound dressings with good mechanical properties, oxygen diffusion properties and biodegradability [13].

In the present study, specialized extraction equipment to optimize removal of contaminating sericin (the glue-like proteins found on the exterior of native silkworm fibers) was developed to address concerns due to inflammation responses to sericin [12]. The remaining core fibers consisting of the fibroin proteins were characterized for mechanical properties and surface morphology and a theoretical model was developed to predict material properties when the fibers organized into a wire-rope geometry. The model accurately predicated matrix mechanical properties for high pitch angle geometries verifying its utility as a research tool. However, the model, as designed, did not account for internal friction within the matrix as the number of twists increases. Therefore, theoretical predictions were expected to be higher than empirical data, as was observed for linear stiffness beyond ~ 2 tw/cm (Fig. 4b). Model enhancements are underway to fit predictions to empirical data given the unknown internal coefficient of friction for the extracted silk fibroin.

The developed 6-cord silk wire-rope matrix possessed mechanical properties similar to that of the native human ACL based on UTS, linear stiffness, yield point and percent elongation at break (Table 1, Fig. 6) [38]. Native human ACL properties vary depending on several factors including patient age and testing conditions [38]; UTS and stiffness for human ACLs from young adults ranging in age from 22 to 35 years were 2160 ± 157 N and 242 ± 28 N/mm, respectively (Table 1). Extrapolated from stress–strain curves provided in the literature [38], the yield point and percent elongation at break were approximately 1200 N and 33%, respectively. When considering a material for use as an ACL replacement, the entire stress–strain curve must be considered in its design. For example, the yield point or force at which a material enters into permanent plastic deformation, is critical to mirror in a prothetic's design; a low prosthetic yield point compared to the native ACL would potential "sprain" or permanently deform the prosthesis in vivo under physiological loading regimes normally sustained by a functional ACL.

Fatigue analysis was performed in only saline without a serum lubricant; fetal calf serum used in vitro, will help to reduce the coefficient of friction between fibers under cyclic loading. Regression analysis of the data, when extrapolated to repetitive physiological load levels of 400 N, indicated an expected matrix lifetime in excess of 3 million cycles or approximately 1 year in vivo to matrix failure. The silk fibers also maintained tensile integrity in tissue culture over 3 weeks (Fig. 7) indicating

their potential to serve as a substrate when dynamic loads are used, such as in some bioreactors. In related experiments (data not shown) collagen fibers from two manufactures failed to maintain mechanical integrity after 1 week in equivalent culture conditions.

Apart from mechanical requirements, biocompatibility and porosity are critical issues for these fiber matrices. Biocompatibility of silk-based materials has been explored recently with a number of different cell types, including transformed fibroblast cell lines [13], osteoblasts [11], primary ACL fibroblasts, human and goat BMSCs, and macrophages (unpublished data), as well as with interactions between fibroin and humoral components of the immune system [12]. In all cases, as long as the sericin is properly extracted, the core fibroin appears to be biocompatible. That is to say the extracted fibroin will not induce a mediated T-cell response in vivo [39] and can support cell attachment, differentiation and tissue formation in vitro if properly prepared. In the present study the silk matrix supported BMSC attachment, spreading along the long axis of the fibers, cell proliferation and ligament specific marker expression in vitro (Fig. 9 and 10).

SEM indicated gaps between individual fibroin filaments of $\sim$5–60 μm (Fig. 8A). As such, it is expected that cells can penetrate between individual fibers if properly stimulated. This conclusion is supported in the literature where fibroblasts stimulated as part of a granulosous response to silk suture infiltrated fibers to encapsulate individual fibroin filaments [33,34]. Matrix porosity and appropriate cell infiltration is a critical step in generating a functional ACL prosthesis in vitro. However, it appears with the current seeding methodology and matrix geometry, cells initially get held up at the surface of the matrix and are not induced (e.g., perfusion) to infiltrate the interior of individual bundles. Spreading of these cells (Fig. 8C&D) then walls off the interior of the matrix to proliferating cells and developing ECM. Several parameters will be studied in future experiments to enhance infiltration and uniform matrix production including matrix geometry, seeding methodologies (e.g., perfusion, bird-caging of matrix during seeding), and the in vitro growth environment (e.g., mechanical stimulation).

The development of the theoretical model will aid in the generation of several matrices of varying geometries with desired mechanical properties. For example, a future matrix may contain only two levels of hierarchy by increasing the number of cords that comprise the final matrix. This will likely increase the ratio of surface area to volume for cell seeding and collagenous ingrowth. The development of an advanced bioreactor system that combines perfusion through and sheath flow around the matrix while allowing direction mechanical manipulation of the matrix (e.g., translational and rotational strains) is under development and will provide alternative cell seeding methodologies.

The fibroin supported baseline levels of ligament specific marker expression including collagen types I and III and tenascin-C (Fig. 10), and did not promote the upregulation of the non-specific markers bone sialoprotein or collagen type II, indicators of bone or cartilage differentiation, respectively. Furthermore, the 8.9 ratio of collagen type I to collagen type III expression was physiologically relevant when compared to native human ACLs [17] and therefore, not indicative of a wound healing response, i.e., non-excessive expression of collagen type III [40]. In comparison to human BMSCs grown in collagen gels for 14 days in a static environment [8], baseline levels of collagen types I and III and tenascin-C expression on the silk matrix were, respectively, 6.1, 8.2 and 7.6 fold greater.

The matrix described in the present study demonstrates that an appropriate biomaterial based on silk can be designed and engineered for specific tissue targets based on required mechanical properties. The wire-rope design provided an 80% decrease in matrix stiffness to physiological levels without sacrificing strength when compared to an equivalent matrix of parallel fibroin fibers (Table 1). Values provided in Table 1 for an equivalent parallel matrix (i.e., assuming an equal number of fibers to the 6-cord matrix) were predicted from the properties of a single extracted fiber (Fig. 3) multiplied by 3240 (the final number of fibers in the twisted 6-cord matrix). Given the low number of tw/cm of the 6-cord matrix at the bundle and strand level (e.g., 2 tw/cm), Fig. 4a predicts only a slight drop in UTS. However, the large decrease in stiffness predicted from a parallel to twisted matrix (Table 1) suggests that (1) the wire-rope design of the 6-cord matrix either helped to incorporate or group individual fibers together to act as a single larger fiber increasing matrix UTS or (2) the UTS of a single fiber (derived from the testing of 10 fibers in parallel) was underestimated due to either slippage between the individual fibers or non-uniform distribution of tension throughout the bundle of 10 parallel fibers.

This successful ability of the wire-rope design to decrease stiffness to physiological levels without sacrificing UTS was a direct result of the extraordinary high ultimate tensile stress (N/mm^2) of silk fibers. Furthermore, the high ultimate stress of the 6-cord matrix allows the entire structure to fit within a 4.0 mm bone tunnel and occupy only 99 mm^3 of space (given a 27 mm length); compared to an ACL with average diameter of 8 mm and length of 27 mm, the silk would occupy only 7.3% of the intra-articular space from tibia to femur. Therefore, the silk fiber matrix occupying less space than the ACL can initially provide an equivalent stabilizing function in vivo. As a result, the 6-cord matrix is smaller in diameter, provides greater void volume leaving room

for host tissue ingrowth and decreases mass transfer limitations when compared to traditional ACL grafts (e.g., autologous single cord patellar tendon, a 2 or 4-cord hamstring graft, and allografts).

The support of host tissue ingrowth must not promote stress-shielding of the developing matrix in vivo. The matrix must adequately communicate environmental signals to the developing tissue, mediated by the cells, in order for the correct extracellular matrix organization to be achieved and assume the role as the main stabilizer of the ACL. The ability to design for matrix stiffness to desired levels (Table 1) will ensure stress-shielding is observed in vivo. However, the optimal initial matrix stiffness must be determined experimentally and will be dependent on the host response to the tissue engineered ACL as well as the rates of tissue ingrowth and silk degradation in vivo. For example, patellar tendon grafts provide the best surgical outcome to date due to their bone-to-bone fixation; however, the patellar–tendon graft used for reconstruction is initially three times stiffer than a native ACL: 685 ± 86 N/mm [41].

The mechanical integrity of silk during cell culture, the ability to support hBMSCs attachment, spreading and growth as a reflection of the biocompatibility of these protein fibers, and the ability to design for matrix stiffness and strength through the wire-rope geometry to match specific host tissue mechanical profiles, suggest that silk fibroin matrices provide an important new option in scaffolding for a variety of biomaterial and tissue engineering needs, including the ACL. Studies are currently in progress to optimize hBMSC ligament specific differentiation in vitro utilizing a physiologically relevant mechanical regime in a bioreactor system and the silk fibroin matrices as scaffolds.

Acknowledgements

Support for various parts of this work from the NSF (DMR, BES), the NIH (NIDR), the Liebmann Foundation, and Tissue Regeneration Inc., is gratefully acknowledged. We would like to thank the New England Medical Center (Boston, MA) for their generous supply of sutures.

References

[1] Tsuda E, Okamura Y, Ishibashi Y, Otsuka H, Toh S. Techniques for reducing anterior knee symptoms after anterior cruciate ligament reconstruction using bone–patellar tendon–bone autograft. Am J Sports Med 2001;29:450–6.

[2] Fu FH, Bennett CH, Ma B, Menetrey J, Lattermann C. Current trends in anterior cruciate ligament reconstruction, Part II. Operative procedures and clinical correlations. Am J Sports Med 2000;28:124–30.

[3] Corry IS, Webb JM, Clingeleffer AJ, Pinczewski LA. Athroscopic reconstruction of the anterior cruciate ligament, a comparison of patellar tendon autograft and four strand hamstring tendon autograft. Am J Sports Med 1999;27:444–54.

[4] Otto D, Pinczewski LA, Clingeleffer A, Odell R. Five-year results of single-incision anterior cruciate ligament reconstruction with patellar tendon autograft. Am J Sports Med 1998;26: 181–8.

[5] Langer R, Vacanti J. Tissue engineering. Science 1993;260: 920–6.

[6] O'Connor JT, Shercliff D, FitzPatrick J, Bradley DM, Daniel E, Biden J, Goodfellow J. Geometry of the knee. In: Daniel D., et al., editors. Knee ligaments: structure, function, injury and repair. New York: Raven Press, 1990. p. 163–99.

[7] Woo SL-Y, Adams DJ. The tensile properties of human anterior cruciate ligament (ACL) and ACL graft tissues. In: Daniel D et al., editors. Knee ligaments: structure, function, injury and repair. New York: Raven Press, 1990. p. 279–89.

[8] Altman GH, Horan RL, Martin I, Farhadi J, Stark PRH, Volloch V, Richmond JC, Vunjak-Novakovic G, Kaplan D. Cell differentiation by mechanical stress. FASEB J 2001, 10.1096/fj.01-0656fje.

[9] Inouye K, Kurokawa M, Nishikawa S, Tsukada M. Use of Bombyx mori silk fibroin as a substratum for cultivation of animal cells. J Biochem Biophys Meth 1998;37:159–64.

[10] Greenwald D, Shumway S, Albear P, Gottlieb L. Mechanical comparison of 10 suture materials before and after in vivo incubation. J Surg Res 1994;56(4):372–7.

[11] Sofia S, McCarthy MB, Gronowicz G, Kaplan DL. Functionalized silk-based biomaterials for bone formation. J Biomed Mater Res 2001;54:139–48.

[12] Santin M, Motta A, Freddi G, Cannas M. In vitro evaluation of the inflammatory potential of the silk fibroin. J Biomed Mater Res 1999;46:382–9.

[13] Minoura N, Tsukada M, Nagura M. Physico-chemical properties of silk fibroin membrane as a biomaterial. Biomaterials 1990;11:430–4.

[14] Costello GA. Theory of wire rope. Berlin: Springer, 1997.

[15] Martin I, Jakob M, Schaefer D, Dick W, Spagnoli G, Heberer M. Quantitative analysis of gene expression in human articular cartilage from normal and osteoarthritic joints. Osteoarthritis Cartilage 2001;9:112–8.

[16] Chen EH, Black J. Materials design analysis of the prosthetic anterior cruciate ligament. J Biomed Mater Res 1980;14: 567–86.

[17] Amiel D, Frank C, Harwood F, Fronek J, Akeson W. Tendons and ligaments: a morphological and biochemical comparison. J Orthop Res 1984;1:257–65.

[18] Fu FH, Bennett CH, Lattermann C, Ma CB. Current trends in anterior cruciate ligament reconstruction, Part I. Biology and biomechanics of reconstruction. Am J Sports Med 1999;27: 821–30.

[19] Bosch U, Gassler N, Decker B. Alterations of glycosaminoglycans during patellar tendon autografts healing after posterior cruciate ligament replacement, a biomechanical study in a sheep model. Am J Sports Med 1998;26:103–8.

[20] Shino K, Oakes BW, Horibe S, Nakata K, Nakamura N. Collagen fibril populations in human anterior cruciate ligament allografts. Am J Sports Med 1995;23:203–9.

[21] McCarthy DM, Tolin BS, Schwenderman L. The anterior cruciate ligament: current and future concepts. New York: Raven Press Ltd., 1993. p. 343–56.

[22] Richmond JC, Manseau CJ, Patz R, McConville O. Anterior cruciate reconstruction using a dacron ligament prosthesis. A long-term study. Am J Sports Med 1992;20:24–8.

[23] Lopez-Vazquez E, Juan JA, Vila E, Debon J. Reconstruction of the anterior cruciate ligament with a Dacron prosthesis. J Bone Jt Surg 1991;73:1294–300.
[24] Dunn MG, Tria AJ, Kato YP, Bechler JR, Ochner RS, Zawadsky JP, Silver FH. Anterior cruciate ligament reconstruction using a composite collagenous prosthesis. A biomechanical and histologic study in rabbits. Am J Sports Med 1992;20:507–15.
[25] Dunn MG, Bellincampi LD, Tria AJ, Zawadsky JP. Preliminary development of a collagen-PLA composite for ACL reconstruction. J Appl Polym Sci 1997;63:1423–8.
[26] Weadock KS, Miller EJ, Keuffel EL, Dunn MG. Effect of physical crosslinking methods on collagen-fiber durability in proteolytic solutions. J Biomed Mater Res 1996;32:221–6.
[27] Weadock KS, Miller EJ, Bellincampi LD, Zawadsky JP, Dunn MG. Physical crosslinking of collagen fibers: comparison of ultraviolet irradiation and dehydrothermal treatment. J Biomed Mater Res 1995;29(11):1373–9.
[28] Kato YP, Dunn MG, Zawadsky JP, Tria AJ, Silver FH. Regeneration of Achilles tendon with a collagen tendon prosthesis. Results of a one-year implantation study. J Bone Jt Surg, Am Vol 1991;73:561–74.
[29] Lam KH, Nijenhuis AJ, Bartels H, Postema AR, Jonkman MF, Pennings AJ, Nieuwenhuis P. Reinforced poly(l-lactic acid) fibers as suture material. J Appl Biomater 1995;6:191–7.
[30] Rossitch Jr. E , Bullard DE, Oakes WJ. Delayed foreign-body reaction to silk sutures in pediatric neurosurgical patients. Childs Nerv Syst 1987;3:375–8.
[31] Soong HK, Kenyon KR. Adverse reactions to virgin silk sutures in cataract surgery. Ophthalmology 1984;91:479–83.
[32] Bucknall TE, Teare L, Ellis H. The choice of a suture to close abdominal incisions. Eur Surg Res 1983;15:59–66.
[33] Salthouse TN, Matlaga BF, Wykoff MH. Comparative tissue response to six suture materials in rabbit cornea, sclera, and ocular muscle. Am J Ophthalmol 1977;84:224–33.
[34] Postlethwait RW. Long-term comparative study of nonabsorbable sutures. Ann Surg 1970;171:892–8.
[35] Asakura T, Demura M, Date T, Miyashita N, Ogawa K, Williamson MP. NMR study of silk I structure of *Bombyx mori* silk fibroin with N-15- and C-13-NMR chemical shift contour plots. Biopolymers 1997;41:193–203.
[36] Cunniff J, Fossey S, Song J, Auerbach M, Kaplan DL, Eby R, Adams W, Vezzie D. Mechanical and thermal properites of Nephila clavipes dragline silk. Polym Adv Technol 1994;5:401–10.
[37] Winkler S, Wilson D, Kaplan DL. Controlling beta-sheet assembly in genetically engineered silk by enzymatic phosphorylation/dephosphorylation. Biochemistry 2000;39(41):12739–46.
[38] Woo SL-Y, Hollis JM, Adams DJ, Lyon RM, Takai S. Tensile properties of human femur–anterior cruciate ligament–tibia complex: the effects of specimen age and orientation. Am J Sports Med 1991;19:217–25.
[39] Kurosaki S, Otsuka H, Kunitomo M, Koyama M, Pawankar R, Matumoto K. Fibroin allergy. IgE mediated hypersensitivity to silk suture materials. Nippon Ika Daigaku Zasshi—J Nippon Med Sch 1999;66:41–4.
[40] Arnoczky SP, Matyas JR, Buckwalter JA, Amiel D. Anatomy of the anterior cruciate ligament. In: Jackson DW, editor. The cruciate ligament-current and future concepts. New York: Raven Press, 1993.
[41] Noyes FR, Butler Dl, Grood ES, et al. Biomechanical analysis of human ligament grafts used in knee-ligament repairs and reconstruction. J Bone Jt Surg Am 1984;66:344–52.